PHOTOSYNTHETICA
International Journal for Photosynthesis Research

DOI 10.32615/ps.2021.043 PHOTOSYNTHETICA 59 (4): 693-701, 2021

Evaluation of the photosynthetic characteristics of upland cotton (*Gossypium hirsutum* L.) germplasm based on chlorophyll *a* fluorescence

Y. SUN[*], X.M. XU[**], Y.H. JIA[***], W.Q. DONG[*], X.M. DU[***,+], H.Q. DENG[#,+], and C.M. TANG[*,+]

State Key Laboratory of Crop Genetics and Germplasm Enhancement, College of Agriculture, Nanjing Agricultural University, 210095 Nanjing, Jiangsu, China[*]
Colleges of Life Science, Nanjing Agricultural University, 210095 Nanjing, Jiangsu, China[**]
State Key Laboratory of Cotton Biology, Institute of Cotton Research of CAAS, 455000 Anyang, Henan, China[***]
Taicang Cotton Breeding Center, Taicang, Jiangsu, China[#]

Abstract

Handy Plant Efficiency Analyser (*Handy PEA*) provides a method for the high-throughput screening of photosynthetic germplasm. However, the large number of chlorophyll *a* fluorescence parameters (CFPs) from *PEA* and the inconsistency of CFP applications among studies greatly limit the accuracy of photosynthesis analyses. In this study, all 53 CFPs of 186 upland cotton cultivars (strains) were measured at 12:00 and 17:00 h. Thirty-two CFPs were selected according to biological importance, and the CFP relationships were determined. Differences in the response ability of cotton cultivars (strains) to high light intensity stress were demonstrated by the distribution of CFPs. Furthermore, the classification and evaluation of photosynthetic characteristics of cotton cultivars (strains) were carried out by Principal Component Analysis and Cluster Analysis. Finally, ten cotton cultivars (strains) with good photosynthetic performance were selected. This study provides a high-throughput method how to identify cotton germplasm resources with high photosynthetic efficiency.

Keywords: chlorophyll *a* fluorescence parameter; *Handy PEA*; upland cotton germplasm.

Introduction

Various germplasm resources with genetic diversity are the basis of breeding. The identification of germplasm resources is an important aspect of breeding. Photosynthetic product accumulation is the basis of crop growth and development (Long *et al.* 2006, Zhu *et al.* 2012). Therefore, it is important to evaluate germplasm resources with different photosynthetic activities.

Chlorophyll *a* fluorescence (CF) is a reliable, popular and high-throughput tool for use in photosynthesis research (Stirbet *et al.* 2018). CF signals contain rich photosynthesis information and may be widely used to quickly monitor the state of leaf photosynthesis in plants under stress (Sonobe *et al.* 2018), such as temperature (Rapacz 2007, Stefanov *et al.* 2011), moisture (Tsonev *et al.* 2011), salt (Gonzalez-Mendoza *et al.* 2011), nutrient elements (Kalaji *et al.* 2018), plant senescence (Cordon

Highlights

- *Handy PEA* was used to evaluate the photosynthetic characteristics of 186 cotton germplasm resources at high throughput
- Out of total 53 chlorophyll *a* fluorescence parameters, 32 were selected according to their biological importance
- Finally, ten cotton cultivars (strains) with excellent photosynthetic characteristics were selected

Received 22 July 2021
Accepted 8 September 2021
Published online 16 December 2021

[+]Corresponding authors
e-mail: duxiongming@caas.cn (X.M. Du)
tangcm@njau.edu.cn (C.M. Tang)

Abbreviations: 10RC/ABS – optical reaction centre coefficient; ABS – absorbed light energy; CA – Cluster Analysis; CF – chlorophyll *a* fluorescence; CFPs – chlorophyll *a* fluorescence parameters; CS – unit exposed area; ET_0 – energy of light of PSII used to transmit electrons; KMO – Kaiser-Meyer-Olkin; PC – principal component; PCA – Principal Component Analysis; RE_0 – energy of light of PSI used to transmit electrons; TR_0 – captured light energy which is used to restore Q_A.
Conflict of interest: The authors declare that they have no conflict of interest.

et al. 2016), and pathogen infection (Barón *et al*. 2016, Ivanov and Bernards 2016).

Although CFPs can be used to evaluate plant photosynthesis rapidly and efficiently, there are numerous parameters, and most studies only select a few (Juneau *et al*. 2007). F_v/F_m was used to investigate the effect of warming and drought on the CFPs of dominant species of Mediterranean shrubland (Prieto *et al*. 2009). The change in photosynthesis under salt stress in rapeseed was investigated with ten CFPs, such as ET_0/ABS, F_0, F_v, F_m, F_v/F_m, $PI_{(abs)}$, φ_{Eo}, RC/ABS, φ_{Do}, and ψ_0 (Bacarin *et al.* 2011). The natural ageing of leaves was examined using five CFPs, ET_0/CS_0, F_v/F_m, F_0, F_m, and $PI_{(abs)}$ (Li *et al.* 2009). The selection of limited CFPs for analyses limits the accuracy of the interpretation of the photosynthetic activity.

Principal Component Analysis (PCA) aims to use the concept of 'dimension reduction' to transform multiple indices into a few comprehensive indices. PCA is an effective method for in-depth analysis of JIP-test fluorescence parameters. The hidden information in the large data of the fluorescence parameters can be identified using PCA (Goltsev *et al.* 2012).

The present study examined 53 CFPs of 186 upland cotton cultivars (strains) (the germplasms were provided by the Institute of Cotton Research of CAAS) that were evaluated at noon (the plants were exposed to high-light intensity stresses leading to depression of photosynthesis at 12:00 h) and 17:00 h (the plants were not subjected to high-intensity stresses at 17:00 h) using *PEA* (Maai *et al.* 2020). The cotton cultivars (strains) were classified and evaluated by PCA and Cluster Analysis (CA). A method for high-throughput analysis of the photosynthetic potential of upland cotton germplasms was established.

Materials and methods

Plant materials: A total of 186 upland cotton cultivars (strains) were included in the study, the names of which are provided in Table 1S (*supplement*).

Chl *a* fluorescence measurement: A total of 186 cotton cultivars (strains) were grown in an experimental field under natural conditions in Anyang, China, in August 2012. Cotton cultivars (strains) were planted according to the management method of field production. During the flowering period of cotton, fluorescence data were measured at 12:00 and 17:00 h using a *Handy PEA* (*Hansatech Instruments Ltd.*, Norfolk, UK) according to Strasser *et al*. (2001). Leaves of upland cotton cultivars (strains) were kept in the dark for at least 30 min. After dark treatment, Chl *a* fluorescence induction curves were measured using *PEA* with red irradiance of 3,000 μmol(photon) m^{-2} s^{-1}. Measurements were repeated six times for each cultivar (strain). The significance of CFPs is shown in Table 1. Measurements were performed at 12:00 and 17:00 h on the same day. The results in our study are valid for the same or a similar climate. Each upland cotton cultivar (strain) had optimal growing conditions and the obtained results may be different under other climatic conditions.

Data analysis: Measured signals were analysed using *Biolyzer 4HP* software *version 4.0.30.03.02* according to the JIP-test. The extracted parameters (F_0, F_1, F_2, F_3, F_4, F_5, and F_m) were calculated to derive all 53 CFPs (*see* Appendix).

Statistical analysis: The calculation of the median, interquartile range, mean, and *Mann-Whitney*'s *U* test of CFPs at 12:00 and 17:00 h was performed by *Excel 2013* and *SPSS 19.0*. The data of 186 cultivars (strains) of 32 parameters were input into *SPSS 19.0*, and the PCA was performed by 'Analysis – Data reduction – Factor – Principal components'. Principal components of PCA were put into *OriginPro 2021* for UPGMA of system clustering.

Results

Selection of CFPs: A total of 53 CFPs were derived from the *PEA*. F_1, F_2, F_3, F_4, F_5, F_m, V_I, and V_J are the points representing the fluorescence intensity on the OJIP kinetics curve. dV/dT_0 and dVG/dT_0 represent the slope of the OJIP kinetics curve at 300 and 100 s, respectively. These ten parameters have no obvious biological meaning in the evaluation of the photosynthetic performance of germplasm resources.

$SumK = K_p + K_n$, $\varphi_{Po} = 1 - \varphi_{Do}$, $F_0/F_m = \varphi_{Do}$, $F_v/F_m = \varphi_{Po}$. Therefore, SumK, F_0/F_m, F_v/F_0, F_v/F_m, and φ_{Do} were eliminated, but K_p, K_n, and φ_{Po} were retained.

Due to the existence of δ_{Ro}, ψ_0, φ_{Po} and ABS/RC, the CFPs $\delta_{Ro}/(1 - \delta_{Ro})$, $\psi_0/(1 - \psi_0)$, $\varphi_{Po}/(1 - \varphi_{Po})$, D.F., and 10RC/ABS were removed from evaluating cotton photosynthesis due to their relative redundancy. Finally, 32 CFPs were selected for follow-up analysis.

Statistical analysis of CFPs: The variations in the 32 CFPs were determined for the leaves of 186 upland cotton cultivars (strains) at 12:00 and 17:00 h. The *Mann-Whitney*'s *U* test showed that four CFPs were insignificantly but 28 CFPs were significantly different between 12:00 and 17:00 h (Table 1). This difference may be due to environmental differences, such as temperature, strong light intensity, and other stresses between 12:00 and 17:00 h. Therefore, it is necessary to measure different times of the day when evaluating the photosynthetic performance of cotton cultivars (strains).

Distribution of CFPs of upland cotton cultivars (strains): At 12:00 h, the distribution range of CFPs of cotton cultivars (strains) was widespread. Moreover, 16 parameters, such as ABS/RC, F_0, ABS/CS_m, TR_0/CS_0, ET_0/CS_0, DI_0/RC, DI_0/CS_0, DI_0/CS_m, φ_{Po}, RE_0/RC, RE_0/CS_0, K_p, K_n, RC/CS_0, N, and S_m/T showed two-peak distribution (Fig. 1S, *supplement*). At 17:00 h, the distribution range of CFPs of cotton cultivars (strains) was narrower. The distribution of CFPs clearly showed that different cotton cultivars (strains) responded differently to high temperature and light intensity at noon.

Table 1. Chlorophyll *a* fluorescence parameters of leaves at 12:00 and 17:00 h in upland cotton cultivars.

Parameter	Median at 12:00 h	Interquartile range at 12:00 h	Mean at 12:00 h	Median at 17:00 h	Interquartile range at 17:00 h	Mean at 17:00 h	*Z*-value	*P*-value
F_0	437.708	160.417	404.013	359.083	47.467	361.423	–2.526	0.012
φ_{Po}	0.773	0.053	0.776	0.805	0.026	0.803	–8.608	0.000
φ_{Eo}	0.472	0.474	0.470	0.546	0.043	0.544	–13.890	0.000
φ_{Do}	0.227	0.053	0.224	0.195	0.025	0.197	–8.610	0.000
S_m	33.998	8.404	33.669	35.641	3.991	35.491	–3.371	0.001
N	52.927	18.631	52.304	52.234	5.583	52.159	–0.068	0.945
K_p	1.574	0.810	1.779	1.993	0.330	2.000	–4.327	0.000
K_n	0.486	0.073	0.494	0.483	0.026	0.484	–1.558	0.119
ABS/RC	2.020	0.365	2.009	1.824	0.169	1.840	–7.404	0.000
TR_0/RC	1.565	0.185	1.553	1.473	0.102	1.475	–6.544	0.000
ET_0/RC	0.941	0.129	0.937	1.000	0.064	0.995	–6.588	0.000
DI_0/RC	0.464	0.188	0.457	0.358	0.073	0.364	–8.117	0.000
RE_0/RC	0.625	0.136	0.624	0.503	0.038	0.502	–14.427	0.000
RE_0/CS_0	154.039	57.242	142.871	109.946	11.237	110.699	–9.826	0.000
RC/CS_0	233.774	44.198	227.175	221.489	15.081	221.217	–2.675	0.007
TR_0/CS_0	373.652	110.062	353.700	325.162	32.569	325.796	–2.705	0.007
ET_0/CS_0	226.381	69.006	213.128	219.225	14.779	219.590	–0.313	0.754
DI_0/CS_0	112.144	64.771	105.590	79.359	20.860	80.641	–6.090	0.000
$PI_{(abs)}$	2.790	1.457	2.994	4.961	1.802	5.065	–13.124	0.000
$PI_{(abs,\ total)}$	5.749	1.717	5.966	5.125	1.751	5.220	–4.628	0.000
δ_{Ro}	0.670	0.073	0.667	0.505	0.038	0.504	–16.621	0.000
RC/CS_m	1,017.719	89.570	1,025.545	1,142.762	107.000	1,024.156	–11.210	0.000
ABS/CS_m	2,061.750	302.290	2,040.232	2,077.833	113.330	2,073.044	–1.525	0.127
TR_0/CS_m	1,577.069	143.855	1,581.249	1,673.572	117.305	1,666.846	–8.418	0.000
ET_0/CS_m	965.418	127.750	959.340	1,141.708	122.831	1,130.597	–13.264	0.000
DI_0/CS_m	491.779	173.586	458.983	404.926	53.332	406.198	–3.605	0.000
$SFI_{(ABS)}$	2.344	0.621	2.403	3.002	0.427	2.997	–12.014	0.000
$\phi_{Ro} = RE_0/ABS$	0.313	0.027	0.312	0.278	0.029	0.274	–13.251	0.000
$\rho_{Ro} = RE_0/TR_0$	0.343	0.042	0.402	0.343	0.030	0.341	–14.514	0.000
ψ_0	0.610	0.049	0.604	0.683	0.037	0.676	–14.023	0.000
S_m/T	0.700	0.039	0.081	0.095	0.034	0.093	–6.028	0.000
$PI_{(cso)}$	12,592.638	3,348.985	12,796.436	20,027.908	4,934.000	20,051.311	–14.359	0.000
$PI_{(csm)}$	58,278.458	23,404.115	60,258.038	103,894.035	37,283.424	105,461.129	–13.782	0.000

$PI_{(abs)}$, $PI_{(cso)}$, $PI_{(csm)}$, $SFI_{(ABS)}$, and K_p can synthetically reflect the photochemical activity and photosynthetic structure and function of leaves. They tend to have a low-value distribution at 12:00 h and a high-value distribution at 17:00 h (Fig. 1S). The results showed that photosynthetic performance decreased under high temperature and strong light at noon but increased after high temperature in the afternoon.

ABS/RC, F_0, ABS/CS_m, TR_0/RC, TR_0/CS_0, TR_0/CS_m, DI_0/RC, DI_0/CS_0, DI_0/CS_m and K_n comprehensively reflect the absorption, capture, and dissipation of light energy, which overall tend to have a high-value distribution at 12:00 h and a low-value distribution at 17:00 h (Fig. 1S). ET_0/RC, ET_0/CS_0, and ET_0/CS_m reflect the light energy used for electron transfer, with a low overall distribution at 12:00 h and a high overall distribution at 17:00 h (Fig. 1S). $\varphi_{Eo} = ET_0/ABS$, $\psi_0 = ET_0/TR_0$, and $\varphi_{Po} = TR_0/ABS$ reflect the ratio of the light energy used for electron transfer to the light energy absorbed and captured to the light energy absorbed, respectively, which tends to be low at 12:00 h and high at 17:00 h (Fig. 1S). The distribution of these 16 parameters indicates that the leaf absorbs and captures more light energy at high temperature and light intensity, but less light energy is used for electron transfer and more light energy is used for heat dissipation, whereas the opposite phenomenon occurs after high temperature and light intensity in the afternoon.

δ_{Ro}, $\phi_{Ro} = RE_0/ABS$, $\rho_{Ro} = RE_0/TR_0$, and $PI_{(abs,\ total)}$ tended to have a high-value distribution at 12:00 h and a low-value distribution at 17:00 h (Fig. 1S), indicating that PSI photosynthetic performance was higher at noon and lower in the afternoon.

N, S_m, and S_m/T tend to be low at 12:00 h and high at 17:00 h (Fig. 1S), indicating that the PSII receptor

plastoquinone pool decreased at high temperature at noon and increased after a decrease of high temperatures.

Classification, screening, and evaluation of upland cotton cultivars (strains)

PCA at 12:00 h: PCA was performed on 32 CFPs selected at 12:00 h. The existence of DI_0/RC and DI_0/CS_m caused Kaiser–Meyer–Olkin (KMO) or *Bartlett*'s test for Nonpositive Definite Matrices. Therefore, these two parameters were eliminated. Finally, PCA for 30 CFPs was carried out. KMO>0.5, $P<0.05$, and correlation analysis showed the parameters were suitable for PCA (Table 2; Table 2S, *supplement*). The cumulative variance contribution of the first three principal components from PCA was 86.8%, which covered most of the CFP information. The first principal component provided 54.4% of the parameter information, which had a significant positive correlation with F_0, TR_0/CS_0, DI_0/CS_0, RE_0/CS_0, ABS/RC, ET_0/CS_0, TR_0/RC, RE_0/RC, ABS/CS_m, RC/CS_0, and N and a significant negative correlation with K_p, φ_{Po}, K_n, $SFI_{(ABS)}$, and $PI_{(abs)}$. The first principal component is a comprehensive component including PSII absorption, capture, and dissipation energy and PSI electron transfer. The second principal component provided 25% of the information about the parameters, which had a positive correlation with ψ_0, $PI_{(cso)}$, ET_0/CS_m, and $\phi_{Ro} = RE_0/ABS$. The second principal component includes the energy of PSII electron transfer, the proportion of electron transfer to the light energy of capture, and the proportion of electron transfer to the light energy of PSI. The third principal component provided 7.4% of the information about the parameters. The third principal component had a positive correlation with δ_{Ro} and $\phi_{Ro} = RE_0/ABS$. The third principal component primarily includes the electron transfer capability of PSI (Table 3).

According to the calculated principal component coefficients, a linear combination of principal components y1, y2, and y3 was obtained (Table 3S, *supplement*). The relationship between the principal component and parameters can be inferred from principal component coefficients. The higher y1 is, the greater is the light energy absorbed and captured by PSII. However, higher energy was used for heat dissipation, which led to a lower overall photosynthetic performance. The higher y2 is, the higher are the ratios of the electron transfer energy to the electron transfer energy of PSII and of the electron transfer energy of PSI to the absorption energy. The higher y3 is, the higher is the electron transfer capability of PSI.

CA at 12:00 h: Based on y1, y2, and y3, the cotton cultivars (strains) distribution and phylogenetic tree of the cluster were obtained by the scatter plot and CA (Fig. 1; Fig. 2S, *supplement*). The result showed that at 12:00 h cotton cultivars (strains) were divided into three groups according to their photosynthetic characteristics. Group I consisted of 99 cotton cultivars (strains) that absorb and capture more energy, use less energy for electron transfer, and use more energy for heat dissipation. These cultivars (strains) have a weaker overall photosynthetic capacity. Group II included 86 cotton cultivars (strains). Although the energy absorbed and captured by the leaves was low, that used for electron transfer was high, but that used for heat dissipation was low. The overall photosynthetic capacity was high. Group III included one cotton cultivar (strain), which had low energy absorbed and captured and low energy used for heat dissipation but had high energy used for electron transfer. The overall photosynthetic capacity of the cotton was high. The classification of the photosynthetic characteristics of cotton cultivars (strains) was clearly performed by CA (Table 4S, *supplement*; Fig. 2S).

PCA at 17:00: The existence of DI_0/RC and DI_0/CS_m also caused KMO or *Bartlett*'s test for Nonpositive Definite Matrices. Therefore, the two parameters were eliminated. KMO>0.5, $P<0.05$, and correlation analysis showed 30 parameters were suitable for PCA (Table 4; Table 5S, *supplement*). The cumulative variance contribution of the first three principal components was 84.1%, which covered most of the chlorophyll fluorescence parameters. The first principal component can provide 48.9% of the parameter information, which had a significant positive correlation with $PI_{(abs)}$, $SFI_{(ABS)}$, $PI_{(csm)}$, $PI_{(cso)}$, φ_{Po}, φ_{Eo}, $PI_{(abs, total)}$, ψ_0, K_p, RC/CS_m, and ET_0/CS_m and a significant negative correlation with DI_0/CS_0, F_0, and ABS/RC. It contained PSII absorption, electron transfer, dissipated energy, the proportion of energy used for electron transfer, and a comprehensive composition of PSII and PSI electron transfer. The first principal component is highly comprehensive. The second principal component provided 20.2% of the information on parameters, which was positively correlated with RE_0/CS_0 and ET_0/CS_0. The second principal component contained information such as the energy per unit area used for electron transfer. The third principal component provided 14.9% of the parameter information. The third principal component had a positive correlation with δ_{Ro}, which mainly reflects PSI electron transfer efficiency (Table 5).

According to the calculated principal component coefficients, a linear combination of principal components y1, y2, and y3 was obtained (Table 6S, *supplement*). The higher y1 is, the higher is the proportion of absorbed PSII and captured energy for electron transfer, the smaller is the proportion of heat dissipation and the higher the

Table 2. KMO and *Bartlett*'s test at 12:00 h.

Kaiser-Meyer-Olkin measure of sampling adequacy		0.71
Bartlett's test of sphericity	Approx. chi-square	29,805.173
	df	435
	Sig.	0

Table 3. Component eigenvalues and component matrices of Principal Component Analysis at 12:00 h.

Component	Initial eigenvalues			Parameter	Component		
	Total	Variance [%]	Cumulative [%]		1	2	3
1	16.331	54.437	54.437	Zscore(K_p)	–0.988	0.047	0.060
2	7.500	25.000	79.436	Zscore(F_0)	0.986	0.023	–0.052
3	2.214	7.380	86.816	Zscore(TR_0/CS_0)	0.986	0.037	–0.111
4	1.479	4.930	91.746	Zscore(DI_0/CS_0)	0.977	–0.110	0.001
5	1.210	4.034	95.780	Zscore(RE_0/CS_0)	0.950	0.277	0.121
6	0.519	1.731	97.511	Zscore(φ_{Po})	–0.948	0.227	–0.089
7	0.393	1.309	98.820	Zscore(ABS/RC)	0.940	–0.169	–0.089
8	0.166	0.554	99.374	Zscore(ET_0/CS_0)	0.902	0.389	–0.150
9	0.098	0.327	99.700	Zscore(TR_0/RC)	0.877	–0.128	–0.178
10	0.035	0.117	99.818	Zscore(RE_0/RC)	0.874	0.323	0.217
11	0.020	0.068	99.885	Zscore(ABS/CS_m)	0.871	0.314	–0.327
12	0.013	0.045	99.930	Zscore(K_n)	–0.871	–0.323	0.310
13	0.006	0.020	99.950	Zscore($SFI_{(ABS)}$)	–0.863	0.491	0.024
14	0.005	0.017	99.968	Zscore(RC/CS_0)	0.858	0.153	–0.040
15	0.004	0.013	99.981	Zscore(N)	0.829	0.467	0.158
16	0.003	0.009	99.989	Zscore($PI_{(abs)}$)	–0.822	0.541	–0.030
17	0.001	0.003	99.992	Zscore($PI_{(csm)}$)	–0.695	0.681	–0.137
18	0.001	0.002	99.994	Zscore(TR_0/CS_m)	0.588	0.553	–0.501
19	0.001	0.002	99.996	Zscore(ψ_0)	–0.105	0.912	–0.112
20	0.000	0.001	99.998	Zscore($PI_{(cso)}$)	–0.432	0.872	–0.164
21	0.000	0.001	99.999	Zscore(ET_0/CS_m)	0.294	0.869	–0.374
22	0.000	0.001	99.999	Zscore($\phi_{Ro} = RE_0/ABS$)	0.129	0.820	0.525
23	8.14×10^{-5}	0.000	100.000	Zscore(φ_{Eo})	–0.509	0.799	–0.127
24	6.28×10^{-5}	0.000	100.000	Zscore(S_m)	0.604	0.675	0.298
25	2.92×10^{-5}	9.74×10^{-5}	100.000	Zscore($\rho_{Ro} = RE_0/TR_0$)	0.543	0.649	0.516
26	1.71×10^{-5}	5.70×10^{-5}	100.000	Zscore(RC/CS_m)	–0.483	0.612	–0.197
27	1.24×10^{-5}	4.14×10^{-5}	100.000	Zscore($PI_{(abs, total)}$)	–0.537	0.605	0.489
28	5.34×10^{-6}	1.78×10^{-5}	100.000	Zscore(δ_{Ro})	0.659	–0.052	0.670
29	2.31×10^{-6}	7.70×10^{-6}	100.000	Zscore(S_m/T)	0.198	0.109	0.034
30	3.32×10^{-7}	1.11×10^{-6}	100.000	Zscore(ET_0/RC)	–0.134	–0.119	–0.094

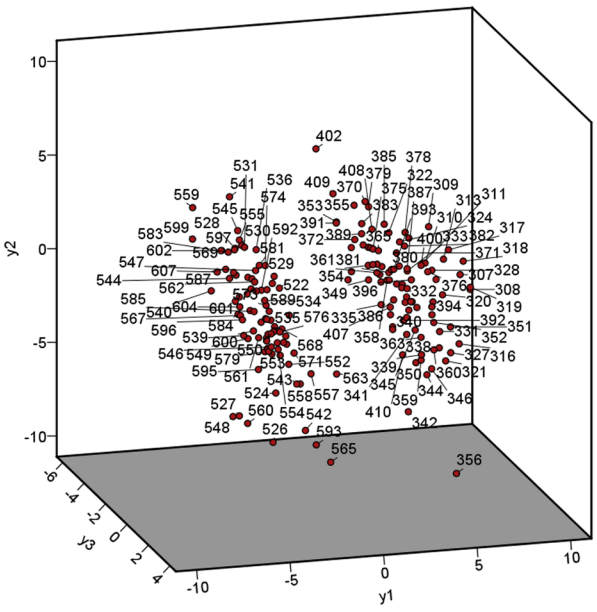

Fig. 1. Clustering of cotton cultivars (strains) at 12:00 h. The markings on the scatter plot are cultivar numbers.

photosynthetic energy utilization ratio. The higher y2 is, the more energy is per unit area of PSII and PSI used for electron transfer. The higher the y3 value is, the higher is the PSI electron transfer efficiency.

CA at 17:00: Based on y1, y2, and y3, the phylogenetic tree of the cluster at 17:00 h was obtained by systematic CA (Fig. 2). The family tree showed that the photosynthetic characteristics of cotton cultivars (strains) were divided into seven groups after high-temperature stress in the afternoon. Group I included 93 cotton cultivars (strains) that had high energy per unit area of PSII and PSI used for electron transfer, but the comprehensive photosynthetic capacity of the cotton cultivars (strains) was low. In Group II, 80 cotton cultivars (strains) were included and their energy per unit area for electron transfer in PSII and PSI in Group II were all moderate, but the photochemical efficiency and comprehensive photosynthetic capacity of

Table 4. KMO and *Bartlett*'s test at 17:00 h.

Kaiser-Meyer-Olkin measure of sampling adequacy		0.674
Bartlett's test of sphericity	Approx. chi-square	30,365.404
	df	435
	Sig.	0

Table 5. Component eigenvalues and component matrix of Principal Component Analysis at 17:00 h.

Component	Initial eigenvalues			Parameter	Component			
	Total	Variance [%]	Cumulative [%]		1	2	3	4
1	14.663	48.876	48.876	Zscore($PI_{(abs)}$)	0.977	–0.097	–0.041	0.000
2	6.072	20.240	69.116	Zscore($SFI_{(ABS)}$)	0.976	–0.088	0.008	0.133
3	4.489	14.963	84.079	Zscore($PI_{(csm)}$)	0.971	–0.014	–0.143	0.013
4	2.570	8.566	92.645	Zscore($PI_{(cso)}$)	0.961	0.090	–0.143	0.044
5	0.996	3.321	95.966	Zscore(φ_{Po})	0.955	–0.089	–0.155	–0.107
6	0.525	1.751	97.716	Zscore(φ_{Eo})	0.948	0.194	–0.040	–0.161
7	0.471	1.570	99.286	Zscore(DI_0/CS_0)	–0.941	0.238	–0.008	0.127
8	0.123	0.410	99.696	Zscore($PI_{(abs, total)}$)	0.930	0.004	0.246	0.167
9	0.033	0.111	99.807	Zscore(K_p)	0.884	–0.404	0.143	–0.142
10	0.029	0.096	99.904	Zscore(ψ_0)	0.880	0.319	0.008	–0.174
11	0.009	0.029	99.933	Zscore(ABS/RC)	–0.840	0.313	–0.026	–0.419
12	0.006	0.019	99.951	Zscore(RC/CS_m)	0.837	0.040	–0.349	0.393
13	0.005	0.016	99.967	Zscore(ET_0/CS_m)	0.831	0.411	–0.352	–0.100
14	0.004	0.012	99.979	Zscore(F_0)	–0.824	0.471	–0.166	0.205
15	0.002	0.008	99.987	Zscore(TR_0/CS_0)	–0.751	0.550	–0.323	0.145
16	0.001	0.003	99.991	Zscore($\phi_{Ro} = RE_0/ABS$)	0.727	0.393	0.524	0.143
17	0.001	0.002	99.993	Zscore(TR_0/RC)	–0.673	0.386	–0.110	–0.604
18	0.001	0.002	99.995	Zscore(ET_0/CS_0)	0.017	0.900	–0.336	–0.014
19	0.001	0.002	99.996	Zscore(RE_0/CS_0)	–0.096	0.895	0.320	0.272
20	0.000	0.001	99.997	Zscore(RE_0/RC)	0.072	0.771	0.563	–0.210
21	0.000	0.001	99.999	Zscore(S_m/T)	–0.374	0.465	0.181	0.290
22	0.000	0.001	99.999	Zscore(δ_{Ro})	–0.116	0.374	0.778	0.374
23	9.59×10^{-5}	0.000	99.999	Zscore(ABS/CS_m)	0.293	0.605	–0.694	0.055
24	5.84×10^{-5}	0.000	100.000	Zscore(K_n)	–0.330	–0.604	0.676	–0.057
25	3.78×10^{-5}	0.000	100.000	Zscore($\rho_{Ro} = RE_0/TR_0$)	0.540	0.494	0.636	0.190
26	2.95×10^{-5}	9.84×10^{-5}	100.000	Zscore(TR_0/CS_m)	0.604	0.436	–0.612	–0.001
27	1.47×10^{-5}	4.90×10^{-5}	100.000	Zscore(S_m)	0.508	0.292	0.603	0.004
28	6.74×10^{-6}	2.25×10^{-5}	100.000	Zscore(N)	0.150	0.515	0.561	–0.317
29	3.24×10^{-6}	1.08×10^{-5}	100.000	Zscore(RC/CS_0)	–0.298	0.305	–0.315	0.824
30	4.10×10^{-7}	1.37×10^{-6}	100.000	Zscore(ET_0/RC)	0.248	0.643	–0.100	–0.682

the cotton cultivars (strains) were high. In Group III, there were two cotton cultivars (strains), the light-utilization efficiency was at the middle level, but the energy per unit area for electron transfer of PSI was relatively high. Group IV included two cotton cultivars (strains) that had middle light-use efficiency and great high energy per unit area for electron transfer in PSII and PSI. Group V included one cotton cultivar (strain), which had low light-use efficiency and electron transfer efficiency of PSI. In Group VI, there were seven cotton cultivars (strains). They had a low comprehensive photosynthetic capacity. Group VII included only one cotton cultivar (strain) that had low energy per unit area of PSII and PSI used for electron transfer (Table S7, *supplement*; Fig. S3, *supplement*).

Selection of cotton cultivars (strains) with high photosynthetic efficiency: Through Principal Component Analysis and Cluster Analysis, ten cotton cultivars (strains) with good photosynthetic performance were selected, including Nongdamian7, Zhong80, E0902, E0904, Emian18, Ekangmian9, Zaoshuchangnong7, Su7036, Suyuan04-3, and MSCO-11 (Table 6). They were all in Cluster II at 12:00 and 17:00 h. At 12:00 h, when they were exposed to high-light intensity stress, the energy absorbed

and captured by leaves was low, that used for electron transfer was high, but that used for heat dissipation was low. In general, the photosynthetic capacity of the cultivars (strains) was high. At 17:00 h, when they were not subjected to high-light intensity stress, the photochemical efficiency and comprehensive photosynthetic capacity of the cotton cultivars (strains) were high.

Discussion

The influence of environment on CFPs of upland cotton cultivars (strains): The environment greatly influences the CFPs of many plants (Poormohammad Kiani *et al.* 2008, Piccotto *et al.* 2011). However, no research on the effects of environments on the variation in CFPs of such a large number of upland cotton cultivars (strains) during the day has been reported. The present study revealed significant differences in CFPs between high light intensity at noon and low intensity in the afternoon. Therefore, it is necessary to select a representative time point in a day when CFPs are used to evaluate the photosynthesis of cotton.

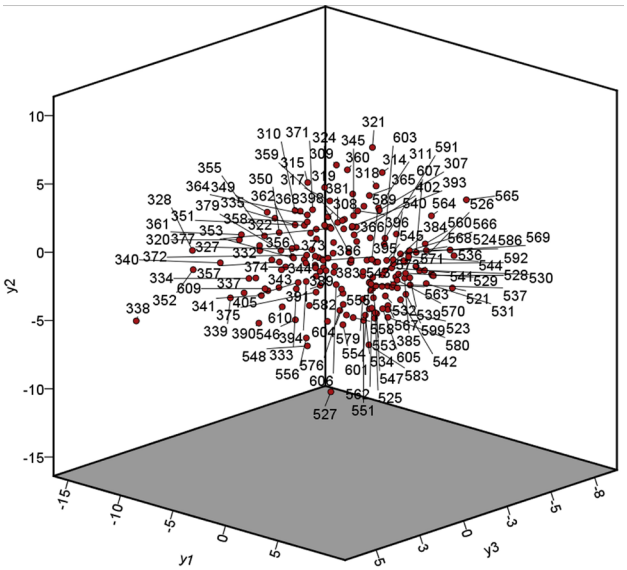

Fig. 2. Clustering of cotton cultivars (strains) at 17:00 h. The markings on the scatter plot are cultivar numbers.

Distribution of CFPs: The range of theoretical values for various CFPs is rarely reported. The list of the distribution of CFPs of the 186 cultivars (strains) provides breeders with ranges of variation between cotton cultivars (strains). The distribution of CFPs at 12:00 and 17:00 h reflected the photosynthetic characteristics of cotton cultivars (strains) under high temperature and high light intensity and after high temperature and high light intensity, which provides breeders with a reference.

Screening of upland cotton germplasm: CFPs have always been used to detect the response of plants to environmental stress (Oukarroum *et al.* 2007). Few researchers use CFPs to screen germplasm resources. Moreover, CFPs are numerous, most researchers usually select several parameters to evaluate the photosynthesis of plants and different studies often choose different parameters. Through analysing all CFPs of a large number of cotton strains, we successfully classified the cotton cultivars (strains), summarized the photosynthetic characteristics of cotton cultivars (strains), and selected the cultivars (strains) with strong photosynthetic performance. Our study provides a quick and efficient method for breeders to select high light efficient cotton germplasm, which greatly benefits breeders.

Conclusion: All CFPs of 186 cotton cultivars (strains) were measured at 12:00 and 17:00 h each day. By using nonparametric tests and frequency distributions, we analysed and compared the photosynthetic characteristics of cotton cultivars (strains) under high temperature and high light intensity at noon and after high temperature and high light intensity in the afternoon. The photosynthetic characteristics of cotton cultivars (strains) were further divided into three groups at 12:00 h and seven groups at 17:00 h by CA, and the photosynthetic characteristics of each cotton group were evaluated. Finally, ten cotton cultivars (strains) with a good photosynthetic performance

Table 6. Top ten upland cotton cultivars (strains) according to Principal Component Analysis and Cluster Analysis.

Cultivar number	Cultivar name	12:00 h			17:00 h		
		y1	y2	y3	y1	y2	y3
530	Nongdamian7	–4.08	2.37	–1.57	8.08	1.31	0.24
531	Zhong80	–5.69	4.09	1.50	7.59	0.08	–0.15
536	E0902	–5.00	3.84	1.38	7.85	1.57	–1.58
537	E0904	–3.53	1.34	0.33	6.79	–0.02	0.29
545	Emian18	–6.26	5.22	1.86	5.77	1.87	1.02
559	Ekangmian9	–6.21	4.08	–2.43	5.72	–0.41	–1.68
562	Zaoshuchangnong7	–4.74	1.77	0.79	7.41	–0.48	2.86
569	Su7036	–5.42	2.46	–1.11	5.80	1.11	–2.59
574	Suyuan04-3	–4.25	2.68	0.92	6.18	0.28	1.53
589	MSCO-11	–4.57	1.81	1.64	5.81	2.32	1.90

at both 12:00 and 17:00 h were selected by PCA. This study provides a method for the identification of cotton germplasm resources with the high photosynthetic efficiency.

References

Bacarin M.A., Deuner S., Silva F.S.P. *et al.*: Chlorophyll *a* fluorescence as indicative of the salt stress on *Brassica napus* L. – Braz. J. Plant Physiol. **23**: 245-253, 2011.

Barón M., Pineda M., Pérez-Bueno M.: Picturing pathogen infection in plants. – Z. Naturforsch. **71**: 355-368, 2016.

Cordon G., Lagorio M.G., Paruelo J.M. *et al.*: Chlorophyll fluorescence, photochemical reflective index and normalized difference vegetative index during plant senescence. – J. Plant Physiol. **199**: 100-110, 2016.

Goltsev V., Zaharieva I., Chernev P. *et al.*: Drought-induced modifications of photosynthetic electron transport in intact leaves: analysis and use of neural networks as a tool for a rapid non-invasive estimation. – BBA-Bioenergetics **1817**: 1490-1498, 2012.

Gonzalez-Mendoza D., Espadas y Gil F., Rodriguez J.F. *et al.*: Photosynthetic responses of a salt secretor mangrove, *Avicennia germinans*, exposed to salinity stress. – Aquat. Ecosyst. Health Manag. **14**: 285-290, 2011.

Ivanov D.A., Bernards M.A.: Chlorophyll fluorescence imaging as a tool to monitor the progress of a root pathogen in a perennial plant. – Planta **243**: 263-279, 2016.

Juneau P., Qiu B., Deblois C.P.: Use of chlorophyll fluorescence as a tool for determination of herbicide toxic effect: Review. – Toxicol. Environ. Chem. **89**: 609-625, 2007.

Kalaji H.M., Bąba W., Gediga K. *et al.*: Chlorophyll fluorescence as a tool for nutrient status identification in rapeseed plants. – Photosynth. Res. **136**: 329-343, 2018.

Li R., Zhou W., Lu W.: [Changes in photosynthesis and chlorophyll fluorescence parameters during rice leaf senescence in low chlorophyll *b* mutant.] – J. Nanjing Agric. Univ. **32**: 10-14, 2009. [In Chinese]

Long S.P., Zhu X.G., Naidu S.L., Ort D.R.: Can improvement in photosynthesis increase crop yields? – Plant Cell Environ. **29**: 315-330, 2006.

Maai E., Nishimura K., Takisawa R., Nakazaki T.: Light stress-induced chloroplast movement and midday depression of photosynthesis in sorghum leaves. – Plant Prod. Sci. **23**: 172-181, 2020.

Oukarroum A., El Madidi S., Schansker G., Strasser R.J.: Probing the responses of barley cultivars (*Hordeum vulgare* L.) by chlorophyll *a* fluorescence OLKJIP under drought stress and re-watering. – Environ. Exp. Bot. **60**: 438-446, 2007.

Piccotto M., Bidussi M., Tretiach M.: Effects of the urban environmental conditions on the chlorophyll *a* fluorescence emission in transplants of three ecologically distinct lichens. – Environ. Exp. Bot. **73**: 102-107, 2011.

Poormohammad Kiani S., Maury P., Sarrafi A., Grieu P.: QTL analysis of CFPs in sunflower (*Helianthus annuus* L.) under well-watered and water-stressed conditions. – Plant Sci. **175**: 565-573, 2008.

Prieto P., Peñuelas J., Llusià J. *et al.*: Effects of long-term experimental night-time warming and drought on photosynthesis, F_v/F_m and stomatal conductance in the dominant species of a Mediterranean shrubland. – Acta Physiol. Plant. **31**: 729-739, 2009.

Rapacz M.: Chlorophyll *a* fluorescence transient during freezing and recovery in winter wheat. – Photosynthetica **45**: 409-418, 2007.

Sonobe R., Wang Q.: Assessing hyperspectral indices for tracing CFPs in deciduous forests. – J. Environ. Manage. **227**: 172-180, 2018.

Stefanov D., Petkova V., Denev I.D.: Screening for heat tolerance in common bean (*Phaseolus vulgaris* L.) lines and cultivars using JIP-test. – Sci. Hortic.-Amsterdam **128**: 1-6, 2011.

Stirbet A., Lazár D., Kromdijk J., Govindjee: Chlorophyll *a* fluorescence induction: Can just a one-second measurement be used to quantify abiotic stress responses? – Photosynthetica **56**: 86-104, 2018.

Strasser R.J, Schansker G., Srivastava A., Govindjee: Simultaneous measurement of photosystem I and photosystem II probed by modulated transmission at 820 nm and by chlorophyll *a* fluorescence in the sub ms to second time range. – In: Proceedings of the 12th International Congress on Photosynthesis, Brisbane, Australia. CSIRO Publishing, Melbourne 2001.

Tsonev T., Velikova V., Yildiz-Aktas L. *et al.*: Effect of water deficit and potassium fertilization on photosynthetic activity in cotton plants. – Plant Biosyst. **145**: 841-847, 2011.

Zhu X.G., Song Q.F., Ort D.R.: Elements of a dynamic systems model of canopy photosynthesis. – Curr. Opin. Plant Biol. **15**: 237-244, 2012.

Appendix. Chlorophyll *a* fluorescence parameters (CFPs).

CFPs	Description
DI_0/CS_m	Dissipated energy flux per CS at t = t_{Fm}
DI_0/CS_0	Dissipated energy flux per CS at t = t_{F0}
DI_0/RC	Dissipated energy flux per RC at t = t_{F0}
dV/dT_0	Net rate of optical reaction centre closure at t = 300 μs
dVG/dT_0	Net rate of optical reaction centre closure at t = 100 μs
ET_0/CS_m	Electron transport flux per CS at t = t_{Fm}
ET_0/CS_0	Electron transport flux per CS at t = t_{F0}
ET_0/RC	Electron transport flux per RC at t = t_{F0}
F_1, F_2, F_3, F_4, and F_5	Fluorescence intensity at 100 μs, 300 μs, 2 ms, 30 ms, and P point, respectively
F_m	Maximum fluorescence, when all PSII RCs are closed
F_0	Minimum fluorescence, when all PSII RCs are open
F_0/F_m	Quantum ratio for thermal dissipation at t = t_{F0}

F_v/F_m	Maximum quantum yield of primary photochemistry
F_v/F_0	PSII potential photochemical activity
K_n	Rate constant of nonphotochemical reaction
K_p	Rate constant of photochemical reaction
N	The number of times Q_A is restored from the beginning of illuminating to the time when it reaches F_m
$PI_{(abs)} = (RC/ABS) \times \varphi_{Po}/(1 - \varphi_{Po}) \times \times \psi_0/(1 - \psi_0)$	Performance index (PI) on absorption basis
$PI_{(abs, total)} = (RC/ABS) \times \varphi_{Po}/(1 - \varphi_{Po}) \times \times \psi_{Eo}/(1 - \psi_{Eo}) \times \delta_{Ro}/(1 - \delta_{Ro})$	Total PI, measuring the performance up to the PSI end electron acceptors
$PI_{(cso)} = RC/CS_0 \times \varphi_{Po}/(1 - \varphi_{Po}) \times \times \psi_0/(1 - \psi_0)$	Performance index on F_0
$PI_{(csm)} = RC/CS_m \times \varphi_{Po}/(1 - \varphi_{Po}) \times \times \psi_0/(1 - \psi_0)$	Performance index on F_m
$SFI_{(ABS)}$	Structural function index
RC/CS_m	Density of RCs (Q_A reducing PSII reaction centres) at $t = t_{Fm}$
$D.F. = \log(PI_{(abs)})$	Photosynthetic driving force
RC/CS_0	Density of RCs (Q_A reducing PSII reaction centres) at $t = t_{F0}$
RE_0/CS_0	Reduction of end acceptors at PSI electron acceptor side per CS at $t = t_{F0}$
ABS/CS_m	Absorption flux per CS at $t = t_{Fm}$
RE_0/RC	Reduction of end acceptors at PSI electron acceptor side per RC at $t = t_{F0}$
ABS/CS_0	Absorption flux per CS at $t = t_{F0}$
S_m	Normalized total complementary area above the OJIP (reflecting multiple turnover Q_A reduction events) or total electron carriers per RC
S_m/T	Reduction rate of plasma plastoquinone pool; $SumK = K_p + K_n$ – total rate constant
TR_0/CS_m	Trapped energy flux per CS at $t = t_{Fm}$; TR_0/CS_0 – trapped energy flux per CS at $t = t_{F0}$
TR_0/RC	Trapping flux (leading to Q_A reduction) per RC
V_J	Relative variable fluorescence at the J-step (2 ms)
V_I	Relative variable fluorescence at the I-step (30 ms)
δ_{Ro}	Efficiency with which an electron can move from the reduced intersystem electron acceptors to the PSI end electron acceptors
$\delta_{Ro}/(1 - \delta_{Ro})$	The quantum efficiency of the reduction of end acceptors
$\rho_{Ro} = RE_0/TR_0$	Efficiency with which a trapped exciton can move an electron into the electron transport chain from Q_A^- to the PSI end electron acceptors
$\varphi_{Do} = DI_0/ABS$	Quantum yield at $t = t_{F0}$ for energy dissipation
$\varphi_{Eo} = ET_0/ABS$	Probability (at time 0) that a trapped exciton moves an electron into the electron transport chain beyond Q_A^-
$\varphi_{Po} = TR_0/ABS$	Maximum quantum yield of primary photochemistry at $t = t_{F0}$
$\varphi_{Po}/(1 - \varphi_{Po}) = TR_0/DI_0$	Ratio of captured light energy to dissipated energy
$\Psi_0 = ET_0/TR_0$	Probability of other electron acceptors that captured exciton-transferred electrons to the electronic chain that exceeds Q_A
$\phi_{Ro} = RE_0/ABS$	Quantum yield for the reduction of end acceptors of PSI per photon absorbed
$\psi_0/(1 - \psi_0) = ET_0/(TR_0 - ET_0)$	The ratio of energy over Q_A to dissipated energy when electrons pass Q_A